Communications in Physics, Vol. 32, No. 1 (2022), pp. 77-94
DOI: https://doi.org/10.15625/0868-3166/16022

ONE-LOOP FORM FACTORS FOR $H \to \gamma^* \gamma^*$ IN R_ξ GAUGE

KHIEM HONG PHAN[1,2,†] AND DZUNG TRI TRAN[3,4]

[1] *Institute of Fundamental and Applied Sciences, Duy Tan University, Ho Chi Minh City* 700000*, Vietnam*

[2] *Faculty of Natural Sciences, Duy Tan University, Da Nang City* 550000*, Vietnam*

[3] *University of Science Ho Chi Minh City,* 227 *Nguyen Van Cu, District* 5*, HCM City, Vietnam*

[4] *Vietnam National University Ho Chi Minh City, Linh Trung Ward, Thu Duc District, HCM City, Vietnam*

E-mail: [†]phanhongkhiem@duytan.edu.vn

Received 19 April 2021; *Accepted for publication 21 August 2021*; *Published 5 January 2022*

Abstract. *In this paper, we present general one-loop form factors for $H \to \gamma^* \gamma^*$ in R_ξ gauge, considering all cases of two on-shell, one on-shell and two off-shell for final photons. Analytic results for the form factors are shown in general forms which are expressed in terms of the Passarino-Veltman functions. We also confirm the results in previous computations which are available for the case of two on-shell photons. The ξ-independent of the result is also discussed. We find that numerical results are good stability with varying $\xi = 0, 1$ and $\xi \to \infty$.*

Keywords: one-loop corrections; analytic methods for Quantum Field Theory; dimensional regularization; Higgs phenomenology.

Classification numbers: 03.70.+k; 11.10.-z.

I. INTRODUCTION

In the standard model of particle physics, the Higgs mechanism is proposed to explain for electroweak symmetry breaking. In this mechanism, the Higgs field is introduced, gauge bosons and all matter particles interact with Higgs boson causing of their masses. After the discovery of the standard model-like Higgs boson, one of the main targets at future colliders such as High Luminosity Large Hadron Collider (HL-LHC) [1, 2] and future lepton colliders [3] is to measure the properties of the Higgs boson (H) precisely. All the Higgs decay modes, Higgs boson productions and the couplings of Higgs to fermions, gauge bosons are measured as accurately as possible. From these activities, one may explore the nature of the Higgs sector as well as search for new physics.

Among Higgs decay modes, the decay of Higgs boson into two photons is the most important for several following reasons. First, this arises at first at one-loop diagrams. Therefore, it is sensitive with new physics in which many new heavy particles such as new gauge bosons, heavy fermions and charged scalars may exchange in the loop diagrams of this decay process. As a result, the calculations for one-loop and higher-loop contributions to the decay amplitudes of $H \to \gamma\gamma$ play a key role in controlling the standard model background, constraining new physics parameters. Secondly, one-loop form factors for $H \to \gamma\gamma^*, \gamma^*\gamma^*$ (γ^* presents for a virtual photon) are useful for studying Higgs productions and its properties at $\gamma\gamma, e\gamma$ colliders [4–10]. Last but not least, the decay processes $H \to \gamma^*\gamma \to f\bar{f}\gamma, \gamma^*\gamma^* \to 4$ fermions provide a crucial tool for controlling background for $H \to f\bar{f}\gamma, H \to 4$ fermions at future colliders.

Many calculations for one-loop contributions to $H \to \gamma\gamma$ within the standard model (SM) and its extensions have been presented in [11–25], also in the references therein. More recently, the authors of Ref. [26] has argued that one-loop W boson contributions to $H \to \gamma\gamma$ lead to different expressions in unitary and in general R_ξ gauges. Latter, the results in Ref. [27] confirm again the gauge invariance of $H \to \gamma\gamma$. On the other hand, the Higgs production in two-photon process and one-loop transition form factor for $H \to \gamma\gamma^*$ has been computed in Ref. [5]. Furthermore, the Higgs production at $e^-\gamma$ collision via the process $e^-\gamma \to e^-H \to e^-b\bar{b}$ has been considered in Ref. [6]. To the best of our knowledge, there are not available one-loop form factors for decay channel $H \to \gamma^*\gamma^*$.

In this paper, the detailed calculations for one-loop form factors for $H \to \gamma^*\gamma^*$ in R_ξ gauge are presented, considering all cases of two on-shell, one on-shell and two off-shell for final photons. The analytical results for the form factors are expressed in terms of Passarino-Veltman functions which are presented in standard forms of `LoopTools` [28]. Analytic formulas for these functions are well-known and their numerical evaluations can be generated by using `LoopTools`. In our present paper, analytic results are shown in $R_{\xi=1}$ for $H \to \gamma^*\gamma^*$ and $\gamma\gamma^*$. While one-loop form factor formulas for $H \to \gamma\gamma$ are presented in both 't Hooft-Veltman and general R_ξ gauges. We also verify the previous calculations in the case of two on-shell photons. The ξ-independent of the result is also discussed. We show the numerical checks for one-loop form factors $H \to \gamma\gamma$ with varying $\xi = 0, 1$ and $\xi \to \infty$.

The rest of the paper is as follows: In Sec. II, we present briefly one-loop tensor reduction method. We then present the evaluations in detail for one-loop form factors of Higgs decay into two photons. Analytical results for the form factors with two real photons, one virtual photon, two virtual photons are shown in this section. Conclusions and outlook are devoted in Sec. III. In appendices, Feynman rules and one-loop amplitude for the decay channel are discussed.

II. CALCULATION

In this calculation, we apply the technique for the reduction of one-loop tensor integrals developed in Ref. [29]. In the following section, we describe briefly this approach. In general, one-loop one-, two- and three-point tensor integrals with rank P are defined as:

$$\{A;B;C\}^{\mu_1\mu_2\cdots\mu_P} = \int \frac{d^dk}{(2\pi)^d} \frac{k^{\mu_1}k^{\mu_2}\cdots k^{\mu_P}}{\{D_1;D_1D_2;D_1D_2D_3\}}. \tag{1}$$

In this formula, D_j for $j = 1,2,3$ are the inverse Feynman propagators which are given:

$$D_j = (k+q_j)^2 - m_j^2 + i\rho. \tag{2}$$

Where q_j are defined as $q_j = \sum_{i=1}^{j} p_i$, p_i are external momenta; m_j are internal masses. The reduction formulas for one-loop one-, two-, three-points tensor integrals up to rank $P = 3$ are written explicitly as follows [29]:

$$A^{\mu} = 0, \tag{3}$$
$$A^{\mu\nu} = g^{\mu\nu}\mathbf{A}_{00}, \tag{4}$$
$$A^{\mu\nu\rho} = 0, \tag{5}$$
$$B^{\mu} = q^{\mu}\mathbf{B}_{1}, \tag{6}$$
$$B^{\mu\nu} = g^{\mu\nu}\mathbf{B}_{00} + q^{\mu}q^{\nu}\mathbf{B}_{11}, \tag{7}$$
$$B^{\mu\nu\rho} = \{g,q\}^{\mu\nu\rho}\mathbf{B}_{001} + q^{\mu}q^{\nu}q^{\rho}\mathbf{B}_{111} \tag{8}$$

and

$$C^{\mu} = q_1^{\mu}\mathbf{C}_1 + q_2^{\mu}\mathbf{C}_2 = \sum_{i=1,2} q_i^{\mu}\mathbf{C}_i \tag{9}$$
$$C^{\mu\nu} = g^{\mu\nu}\mathbf{C}_{00} + \sum_{i,j=1,2} q_i^{\mu}q_j^{\nu}\mathbf{C}_{ij} \tag{10}$$
$$C^{\mu\nu\rho} = \sum_{i=1}^{2}\{g,q_i\}^{\mu\nu\rho}\mathbf{C}_{00i} + \sum_{i,j,k=1}^{2} q_i^{\mu}q_j^{\nu}q_k^{\rho}\mathbf{C}_{ijk}. \tag{11}$$

Here we use the short notation $\{g,q_i\}^{\mu\nu\rho} = g^{\mu\nu}q_i^{\rho} + g^{\nu\rho}q_i^{\mu} + g^{\mu\rho}q_i^{\nu}$. In this method, scalar coefficients $\mathbf{A}_{00}, \mathbf{B}_1, \cdots, \mathbf{C}_{222}$ in right hand side of the above relations are so-called Passarino-Veltman functions [28,29]. The analytical results for these functions are well-known and implemented into computer program named `LoopTools` [28] for numerical evaluations.

We turn our attention to apply the above approach for evaluating the decay process $H \to \gamma^*\gamma^*$. Within the standard model, the decay channel in R_ξ consists of fermion loop diagrams (as shown in Fig. 1) and W boson, Goldstone boson, Ghost particles exchanging in the loop diagrams (seen Fig. 2). In theories beyond the standard model, we also consider the charged scalar particles in the one-loop diagrams (described in Fig. 3).

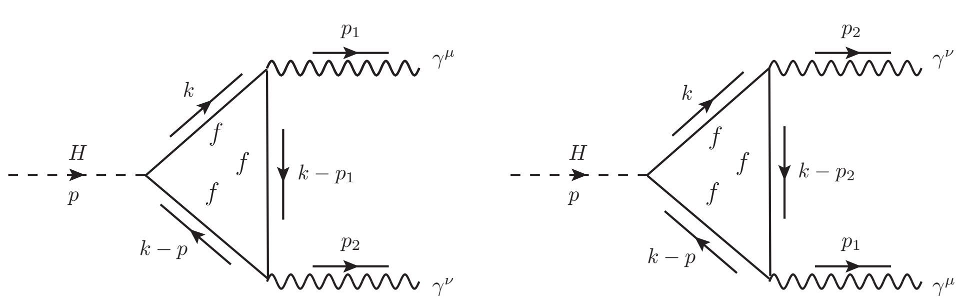

Fig. 1. Fermion loop Feynman diagrams of $H \to \gamma\gamma$ in R_ξ gauge.

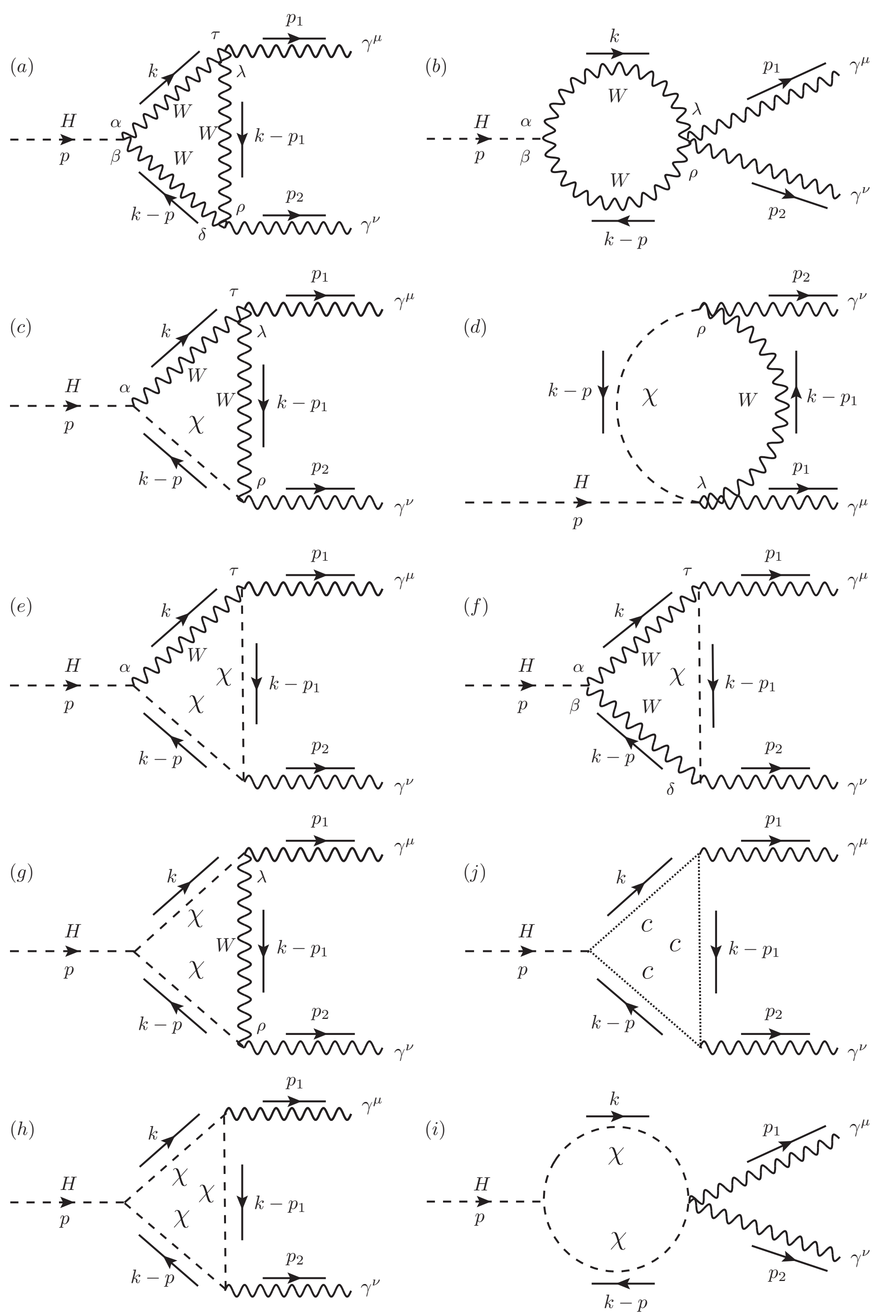

Fig. 2. *W* boson, Goldstone boson, Ghost particles exchanging in the loop diagrams of $H \to \gamma\gamma$ in R_ξ gauge.

In general, the total amplitude of the decay $H \to \gamma^*\gamma^*$ is presented in terms of the Lorentz invariant structure as follows:

$$\mathscr{A}_{H\to\gamma^*\gamma^*} = \frac{e^2 g}{16\pi^2 M_W}\left(\mathscr{A}_{00} g^{\mu\nu} + \mathscr{A}_{21} p_2^{\mu} p_1^{\nu}\right)\epsilon_\mu^*(p_1)\epsilon_\nu^*(p_2). \tag{12}$$

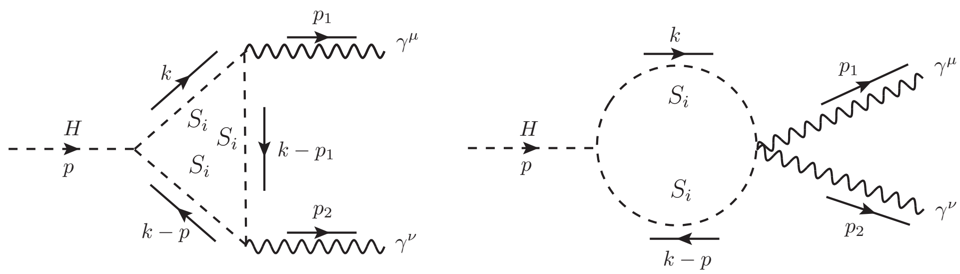

Fig. 3. Charged scalar S_i exchanged in one-loop Feynman diagrams of $H \to \gamma\gamma$ in R_ξ gauge.

The kinematic invariant variables involving the decay channel are

$$p^2 = (p_1 + p_2)^2 = M_H^2, \quad p_1^2 \quad \text{and} \quad p_2^2. \tag{13}$$

In this paper, the form factors $\mathscr{A}_{00}, \mathscr{A}_{21}$ are expressed in terms of Passarino-Veltman functions mentioned in the beginning of this section.

In general R_ξ gauge, in order to simplify the calculations, W boson propagator is decomposed into the following form with a short notation $M_\xi^2 = \xi M_W^2$,

$$\frac{-i}{p^2 - M_W^2}\left[g^{\mu\nu} - (1-\xi)\frac{p^\mu p^\nu}{p^2 - M_\xi^2}\right] = \frac{-i}{p^2 - M_W^2}\left(g^{\mu\nu} - \frac{k^\mu k^\nu}{M_W^2}\right) + \frac{-i}{p^2 - M_\xi^2}\frac{k^\mu k^\nu}{M_W^2}. \tag{14}$$

The first term in the right hand side of this equation is nothing but it is W boson propagator in unitary gauge. While the second term relates to Goldstone boson and Ghost particles.

The calculations are performed with the help of `Package-X` [30] for handling all Dirac traces in d dimensions. The one-loop form factors are then written in terms of Passarino-Veltman functions in standard notations of `LoopTools` [28] on a diagram-by-diagram basis.

II.1. Two off-shell photons

We first present analytic results for one-loop form factors for the decay $H \to \gamma^*\gamma^*$. The notation γ^* is to one off-shell (or a virtual photon). We arrive at the contribution of fermion loop diagrams. Analytic formulas for the form factors are written in terms of Passarino-Veltman functions as

$$\begin{aligned}\mathscr{A}_{00}^{(f)} &= -4m_f^2 N_C Q_f^2\Big\{\mathbf{B}_0\left(M_H^2; m_f^2, m_f^2\right) - 4\mathbf{C}_{00}\left(M_H^2, p_1^2, p_2^2; m_f^2, m_f^2, m_f^2\right)\\ &\quad + \frac{M_H^2 - p_1^2 - p_2^2}{2}\,\mathbf{C}_0\left(M_H^2, p_1^2, p_2^2; m_f^2, m_f^2, m_f^2\right)\Big\},\end{aligned} \tag{15}$$

$$\begin{aligned}\mathscr{A}_{21}^{(f)} &= 4m_f^2 N_C Q_f^2\Big\{4\mathbf{C}_{12}\left(M_H^2, p_1^2, p_2^2; m_f^2, m_f^2, m_f^2\right) + 4\mathbf{C}_{11}\left(M_H^2, p_1^2, p_2^2; m_f^2, m_f^2, m_f^2\right)\\ &\quad + 4\mathbf{C}_1\left(M_H^2, p_1^2, p_2^2; m_f^2, m_f^2, m_f^2\right) + \mathbf{C}_0\left(M_H^2, p_1^2, p_2^2; m_f^2, m_f^2, m_f^2\right)\Big\}.\end{aligned} \tag{16}$$

Here N_C is a color factor ($N_C = 1$ for leptons and $N_C = 3$ for quarks) and $Q_f e$ is electric charge of fermions.

We next consider W boson contributions for the form factors. In general R_ξ gauge, the contributions include W boson, Goldstone boson and Ghost particles in one-loop diagrams. Summing all these diagrams, we get the form factors which are functions of the unphysical parameter ξ and the kinematic invariants $p_1^2, p_2^2, M_H^2, M_W^2$. For illustrating, we only show here the analytic results in 't Hooft-Veltman gauge by taking $\xi = 1$:

$$\begin{aligned}
\mathscr{A}_{00}^{(W)} &= M_W^2\Big\{ -\mathbf{B}_0\left(p_1^2;M_W^2,M_W^2\right) + \mathbf{B}_0\left(p_2^2;M_W^2,M_W^2\right) \\
&\quad +2\left(-4M_H^2+p_1^2+4p_2^2\right)\mathbf{C}_0\left(p_1^2,p_2^2,M_H^2;M_W^2,M_W^2,M_W^2\right)\Big\} \\
&\quad -\left[M_H^2+2(d-1)M_W^2\right]\times \qquad (17)\\
&\quad \times\Big\{\mathbf{B}_0\left(M_H^2;M_W^2,M_W^2\right) - 4\mathbf{C}_{00}\left(p_1^2,p_2^2,M_H^2;M_W^2,M_W^2,M_W^2\right)\Big\}, \\
\mathscr{A}_{21}^{(W)} &= 2M_W^2\Big\{4(d-1)\Big[\mathbf{C}_{22}\left(p_1^2,p_2^2,M_H^2;M_W^2,M_W^2,M_W^2\right) \\
&\quad +\mathbf{C}_{12}\left(p_1^2,p_2^2,M_H^2;M_W^2,M_W^2,M_W^2\right)\Big] \\
&\quad +(4d+2)\mathbf{C}_2\left(p_1^2,p_2^2,M_H^2;M_W^2,M_W^2,M_W^2\right) + 11\mathbf{C}_0\left(p_1^2,p_2^2,M_H^2;M_W^2,M_W^2,M_W^2\right) \\
&\quad +3\mathbf{C}_1\left(p_1^2,p_2^2,M_H^2;M_W^2,M_W^2,M_W^2\right)\Big\} + 4M_H^2\Big\{\mathbf{C}_{22}\left(p_1^2,p_2^2,M_H^2;M_W^2,M_W^2,M_W^2\right) \\
&\quad +\mathbf{C}_{12}\left(p_1^2,p_2^2,M_H^2;M_W^2,M_W^2,M_W^2\right) + \mathbf{C}_2\left(p_1^2,p_2^2,M_H^2;M_W^2,M_W^2,M_W^2\right)\Big\}. \qquad (18)
\end{aligned}$$

For arbitrary extension of the standard models, we have the extra gauge bosons, new heavy fermions and charged scalars which may exchange in the loop diagrams.We extend our calculation directly for these cases by the generalization of coupling of new gauge bosons, heavy fermions and charged scalars to Higgs boson and photons. For an example, by considering the charged scalar particles S_i exchanged in one-loop diagrams, the corresponding amplitude for $H \to \gamma^*\gamma^*$ is

$$\mathscr{A}_{H\to\gamma\gamma}^{(S_i)} = \frac{\lambda_{HS_iS_i} e^2 Q_{S_i}^2}{16\pi^2}\Big(\mathscr{A}_{00}^{(S_i)} g^{\mu\nu} + \mathscr{A}_{21}^{(S_i)} p_2^{\mu} p_1^{\nu}\Big)\epsilon_\mu^*(p_1)\epsilon_\nu^*(p_2). \qquad (19)$$

Applying the same procedure, we derive one-loop form factors due to the contributions of the charged scalar loop diagrams as follows:

$$\begin{aligned}
\mathscr{A}_{00}^{(S_i)} &= -2\Big\{\mathbf{B}_0\left(M_H^2;M_{S_i}^2,M_{S_i}^2\right) - 4\mathbf{C}_{00}\left(M_H^2,p_1^2,p_2^2;M_{S_i}^2,M_{S_i}^2,M_{S_i}^2\right)\Big\}, \qquad (20)\\
\mathscr{A}_{21}^{(S_i)} &= 8\Big\{\mathbf{C}_{12}\left(M_H^2,p_1^2,p_2^2;M_{S_i}^2,M_{S_i}^2,M_{S_i}^2\right) + \mathbf{C}_{11}\left(M_H^2,p_1^2,p_2^2;M_{S_i}^2,M_{S_i}^2,M_{S_i}^2\right) \\
&\quad +\mathbf{C}_1\left(M_H^2,p_1^2,p_2^2;M_{S_i}^2,M_{S_i}^2,M_{S_i}^2\right)\Big\}. \qquad (21)
\end{aligned}$$

By taking the limit of $p_1^2 \to 0$ or $p_2^2 \to 0$, we get the results for the case of one off-shell photon. We refer analytic results for all form factors in which $\gamma(p_1)$ is on-shell photon in appendix A.

II.2. Two on-shell photons

We change our topic to the case of two real photons in the final state of this channel. In this case, on-shell conditions for these photons are implied as

$$p_1^2 = p_2^2 = 0. \tag{22}$$

We then have the relation $p_1 p_2 = M_H^2/2$. Analytic formulas for the form factors are derived as:

$$\begin{aligned}
\mathscr{A}_{00}^{(f)} &= -2m_f^2 N_C Q_f^2 \Big\{ 2\mathbf{B}_0\left(M_H^2; m_f^2, m_f^2\right) - 8\mathbf{C}_{00}\left(M_H^2, 0, 0; m_f^2, m_f^2, m_f^2\right) \\
&\quad + M_H^2 \mathbf{C}_0\left(M_H^2, 0, 0; m_f^2, m_f^2, m_f^2\right) \Big\},
\end{aligned} \tag{23}$$

$$\begin{aligned}
\mathscr{A}_{21}^{(f)} &= 4m_f^2 N_C Q_f^2 \Big\{ 4\Big[\mathbf{C}_{12}\left(M_H^2, 0, 0; m_f^2, m_f^2, m_f^2\right) + \mathbf{C}_{11}\left(M_H^2, 0, 0; m_f^2, m_f^2, m_f^2\right) \\
&\quad + \mathbf{C}_1\left(M_H^2, 0, 0; m_f^2, m_f^2, m_f^2\right) \Big] + \mathbf{C}_0\left(M_H^2, 0, 0; m_f^2, m_f^2, m_f^2\right) \Big\}.
\end{aligned} \tag{24}$$

From one-loop W boson contributions, the analytical results in both 't Hooft-Veltman and general R_ξ gauges are shown. First, the form factors in R_ξ gauge read

$$\begin{aligned}
\mathscr{A}_{00}^{(W)}(\xi) &= \Big[2M_W^2(1-d) - 2M_H^2 - \frac{M_H^4}{2M_W^2} \Big] \mathbf{B}_0(M_H^2; M_W^2, M_W^2) \\
&\quad + \Big[\frac{M_H^4}{M_W^2} + M_H^2(1-\xi) \Big] \mathbf{B}_0(M_H^2; M_\xi^2, M_W^2) \\
&\quad - \Big(\frac{M_H^4}{M_W^2} + 2M_H^2 \Big) \mathbf{B}_1(M_H^2; M_W^2, M_W^2) \\
&\quad + \Big(M_H^2 \xi - \frac{M_H^4}{2M_W^2} \Big) \Big[2\mathbf{B}_1 + \mathbf{B}_0 \Big](M_H^2; M_\xi^2, M_\xi^2) \\
&\quad + \Big[\frac{M_H^4}{M_W^2} + M_H^2(1-\xi) \Big] \Big[\mathbf{B}_1(M_H^2; M_W^2, M_\xi^2) + \mathbf{B}_1(M_H^2; M_\xi^2, M_W^2) \Big] \\
&\quad + [4M_H^2 + 8M_W^2(d-1)] \mathbf{C}_{00}(0, 0, M_H^2; M_W^2, M_W^2, M_W^2) \\
&\quad + \Big[M_H^2 + M_W^2(1-\xi) \Big] \times \\
&\quad \times \Big[2\mathbf{C}_{00}(0, 0, M_H^2; M_W^2, M_W^2, M_\xi^2) - 2\mathbf{C}_{00}(0, 0, M_H^2; M_\xi^2, M_W^2, M_W^2) \\
&\quad + \mathbf{C}_{00}(0, 0, M_H^2; M_W^2, M_\xi^2, M_\xi^2) - \mathbf{C}_{00}(0, 0, M_H^2; M_\xi^2, M_\xi^2, M_W^2) \Big] \\
&\quad + 2M_H^2 M_W^2 \Big[\mathbf{C}_0(0, 0, M_H^2; M_\xi^2, M_W^2, M_W^2) \\
&\quad - \mathbf{C}_0(0, 0, M_H^2; M_W^2, M_W^2, M_\xi^2) - 4\mathbf{C}_0(0, 0, M_H^2; M_W^2, M_W^2, M_W^2) \Big]
\end{aligned}$$

and

$$
\begin{aligned}
\mathscr{A}_{21}^{(W)}(\xi) &= (4M_H^2+8dM_W^2-8M_W^2)\Big[\mathbf{C}_{22}+\mathbf{C}_{12}+\mathbf{C}_2\Big](0,0,M_H^2;M_W^2,M_W^2,M_W^2)\\
&+\Big[M_H^2+M_W^2(1-\xi)\Big]\times\\
&\times\Big[2\mathbf{C}_{22}(0,0,M_H^2;M_W^2,M_W^2,M_\xi^2)-2\mathbf{C}_{22}(0,0,M_H^2;M_\xi^2,M_W^2,M_W^2)\\
&+2\mathbf{C}_{12}(0,0,M_H^2;M_W^2,M_W^2,M_\xi^2)-2\mathbf{C}_{12}(0,0,M_H^2;M_\xi^2,M_W^2,M_W^2)\\
&+\mathbf{C}_{22}(0,0,M_H^2;M_W^2,M_\xi^2,M_\xi^2)-\mathbf{C}_{22}(0,0,M_H^2;M_\xi^2,M_\xi^2,M_W^2)\\
&+\mathbf{C}_{12}(0,0,M_H^2;M_W^2,M_\xi^2,M_\xi^2)-\mathbf{C}_{12}(0,0,M_H^2;M_\xi^2,M_\xi^2,M_W^2)\Big]\\
&+2M_W^2\Big[2\mathbf{C}_1(0,0,M_H^2;M_\xi^2,M_W^2,M_W^2)+\mathbf{C}_1(0,0,M_H^2;M_W^2,M_\xi^2,M_\xi^2) \qquad (25)\\
&+2\mathbf{C}_0(0,0,M_H^2;M_W^2,M_W^2,M_\xi^2)+\mathbf{C}_0(0,0,M_H^2;M_W^2,M_\xi^2,M_\xi^2)\Big]\\
&+\Big[M_H^2+M_W^2(3-\xi)\Big]\times\\
&\times\Big[2\mathbf{C}_2(0,0,M_H^2;M_W^2,M_W^2,M_\xi^2)+\mathbf{C}_2(0,0,M_H^2;M_W^2,M_\xi^2,M_\xi^2)\Big]\\
&+\Big[M_W^2(1+\xi)-M_H^2\Big]\times\\
&\times\Big[2\mathbf{C}_2(0,0,M_H^2;M_\xi^2,M_W^2,M_W^2)+\mathbf{C}_2(0,0,M_H^2;M_\xi^2,M_\xi^2,M_W^2)\Big]\\
&+16M_W^2\mathbf{C}_0(0,0,M_H^2;M_W^2,M_W^2,M_W^2)
\end{aligned}
$$

By setting $\xi=1$, we obtain the results in 't Hooft-Veltman gauge

$$
\begin{aligned}
\mathscr{A}_{00}^{(W)} &= -\left[M_H^2+2(d-1)M_W^2\right]\Big[\mathbf{B}_0\left(M_H^2;M_W^2,M_W^2\right)-4\mathbf{C}_{00}\left(0,0,M_H^2;M_W^2,M_W^2,M_W^2\right)\Big]\\
&-8M_H^2M_W^2\mathbf{C}_0\left(0,0,M_H^2;M_W^2,M_W^2,M_W^2\right), \qquad (26)
\end{aligned}
$$

$$
\begin{aligned}
\mathscr{A}_{21}^{(W)} &= 2M_W^2\Big\{4(d-1)\Big[\mathbf{C}_{22}\left(0,0,M_H^2;M_W^2,M_W^2,M_W^2\right)+\mathbf{C}_{12}\left(0,0,M_H^2;M_W^2,M_W^2,M_W^2\right)\Big]\\
&+2(2d+1)\mathbf{C}_2\left(0,0,M_H^2;M_W^2,M_W^2,M_W^2\right)+11\mathbf{C}_0\left(0,0,M_H^2;M_W^2,M_W^2,M_W^2\right)\\
&+3\mathbf{C}_1\left(0,0,M_H^2;M_W^2,M_W^2,M_W^2\right)\Big\}+4M_H^2\Big[\mathbf{C}_{22}\left(0,0,M_H^2;M_W^2,M_W^2,M_W^2\right) \qquad (27)\\
&+\mathbf{C}_{12}\left(0,0,M_H^2;M_W^2,M_W^2,M_W^2\right)+\mathbf{C}_2\left(0,0,M_H^2;M_W^2,M_W^2,M_W^2\right)\Big].
\end{aligned}
$$

One-loop form factors for this process with the inclusion of charged scalars in the loop diagrams are shown

$$
\mathscr{A}_{00}^{(S_i)} = -2\Big\{\mathbf{B}_0\left(M_H^2;M_{S_i}^2,M_{S_i}^2\right)-4\mathbf{C}_{00}\left(M_H^2,0,0;M_{S_i}^2,M_{S_i}^2,M_{S_i}^2\right)\Big\}, \qquad (28)
$$

$$
\begin{aligned}
\mathscr{A}_{21}^{(S_i)} &= 8\Big\{\mathbf{C}_{12}\left(M_H^2,0,0;M_{S_i}^2,M_{S_i}^2,M_{S_i}^2\right)+\mathbf{C}_{11}\left(M_H^2,0,0;M_{S_i}^2,M_{S_i}^2,M_{S_i}^2\right)\\
&+\mathbf{C}_1\left(M_H^2,0,0;M_{S_i}^2,M_{S_i}^2,M_{S_i}^2\right)\Big\}. \qquad (29)
\end{aligned}
$$

We find that all form factors in $R_{\xi=1}$ in two on-shell photons case can be obtained by taking $p_1^2, p_2^2 \to 0$ from the results in previous subsection.

Table 1. The numerical checks for the form factors in the case of $\xi \to 0, \xi = 1, \xi \to \infty$ are shown. For this check, we set $M_H = 125$ GeV, $M_W = 80.4$ GeV, and $p_1^2 = p_2^2 = 0$ GeV.

diagrams/ξ	$\xi \to 0$	$\xi = 1$	$\xi = 100$	$\xi \to \infty$
a	-3.468876070276491 $+0.044696724580243\,i$	-4.882018101498933	-30.40120343875694	$-2.777777777516398 \cdot 10^{11}$
b	0.4359747855634294 $+1.1775870133864408\,i$	0	22.87057225068166	$2.777777777438721 \cdot 10^{11}$
c	-2.288315292217131 $-0.647907755004331\,i$	-2.345059943153266	-0.5672364405722673	-0.3888888890439217
d	0	0	0	0
e	-1.599294975435531 $-1.787032617316791\,i$	-1.591326628583693	-0.1930905308944328	-0.1666666666694787
f	0.2615610107425627 $+0.8935163086583953\,i$	0	0.04694802196574567	0.08333333330075746
g	0.3357098311660154 $+0.3191403256960426\,i$	0	0.0003307252303052892	$3.357186222008115 \cdot 10^{-14}$
h	-2	0.6243029825430905	0.004041657968703369	$4.028623466417146 \cdot 10^{-13}$
i	0	0	0	0
j	0	-0.12913901976434381	-0.08360295607991542	-0.08333333333336019
Sum	-8.323240710457146	-8.323240710457146	-8.323240710457146	-8.323240710457146

In the limit of $d \to 4$, we confirm previous results, taking Ref. [18] as an example. In detail, our results when $d \to 4$ are presented

$$\begin{aligned}
\mathscr{A}_{00}^{(f)} &= \mathscr{A}_{21}^{(f)} \times \left(-\frac{M_H^2}{2}\right) = \\
&= \frac{m_f^2 N_C Q_f^2}{M_H^2} \left\{ 4M_H^2 + \left(4m_f^2 - M_H^2\right) \ln^2 \left(\frac{-M_H^2 + 2m_f^2 + \sqrt{M_H^4 - 4m_f^2 M_H^2}}{2m_f^2} \right) \right\}
\end{aligned} \tag{30}$$

and

$$\begin{aligned}\mathscr{A}_{00}^{(W)} &= \mathscr{A}_{21}^{(W)} \times \left(-\frac{M_H^2}{2}\right) = \\ &= M_H^2 + 6M_W^2 + \left(\frac{6M_W^4}{M_H^2} - 3M_W^2\right) \ln^2\left(\frac{-M_H^2 + 2M_W^2 + \sqrt{M_H^4 - 4M_H^2 M_W^2}}{2M_W^2}\right).\end{aligned} \tag{31}$$

These results agree with Ref. [18]. We note that the analytic results in different gauges give the same result in Eqs. (30, 31) in the limit $d \to 4$.

Furthermore, we also have analytic results for the form factors due to the charged scalar in the loop at $d = 4$. These factors read

$$\begin{aligned}\mathscr{A}_{00}^{(S_i)} &= \mathscr{A}_{21}^{(S_i)} \times \left(-\frac{M_H^2}{2}\right) = \\ &= \frac{2\lambda_{HS_iS_i} M_W Q_{S_i}^2}{g M_H^2} \left\{ M_H^2 + M_{S_i}^2 \ln^2\left(\frac{-M_H^2 + 2M_{S_i}^2 + \sqrt{M_H^4 - 4M_H^2 M_{S_i}^2}}{2M_{S_i}^2}\right)\right\}.\end{aligned} \tag{32}$$

The ξ-independent of the result is also checked numerically. The numerical results are generated by varying $\xi \to 0$ (is so-called Coulomb gauge), $\xi = 1$ or 't Hooft-Veltman gauge and $\xi \to \infty$ (unitary gauge). In this Table 1, we show the numerical results of

$$(-2/M_H^2) \times \mathscr{A}_{00} = \mathscr{A}_{21}. \tag{33}$$

We find that numerical results show good stability in different gauges.

III. CONCLUSIONS

In this paper, we have presented one-loop form factors for $H \to \gamma^* \gamma^*$ in R_ξ gauge, considering all cases of two on-shell, one on-shell and two off-shell for final photons. Analytic results for the form factors are shown in general forms which are expressed in terms of the Passarino-Veltman functions in stadard notation of `LoopTools`. We have also confirmed the results in previous computations which are available for the case of two on-shell photons. The ξ-independent of the result has also been studied. We find that numerical results are in good stability with varying $\xi = 0, 1$ and $\xi \to \infty$.

ACKNOWLEDGMENT

This research is funded by Vietnam National Foundation for Science and Technology Development (NAFOSTED) under the grant number 103.01-2019.346.

REFERENCES

[1] A. Liss *et al.* [ATLAS], *Physics at a High-Luminosity LHC with ATLAS*, [arXiv:1307.7292 [hep-ex]].
[2] [CMS], *Projected Performance of an Upgraded CMS Detector at the LHC and HL-LHC: Contribution to the Snowmass Process*, [arXiv:1307.7135[hep-ex]].

[3] H. Baer, T. Barklow, K. Fujii, Y. Gao, A. Hoang, S. Kanemura, J. List, H. E. Logan, A. Nomerotski and M. Perelstein, *et al. The international linear collider technical design report - Volume 2: physics*, [arXiv:1306.6352 [hep-ph]].
[4] M. M. Muhlleitner, *Higgs boson search at e^+ e^- and photon linear colliders*, *Acta Phys. Polon. B* **37** (2006) 1127.
[5] N. Watanabe, Y. Kurihara, K. Sasaki and T. Uematsu, *Higgs production in two-photon process and transition form factor*, *Phys. Lett. B* **728** (2014) 202.
[6] N. Watanabe, Y. Kurihara, T. Uematsu and K. Sasaki, *Higgs boson production in e and real γ collisions*, *Phys. Rev. D* **90**(3) (2014) 033015.
[7] M. Melles, W. J. Stirling and V. A. Khoze, *Higgs boson production at the Compton collider*, *Phys. Rev. D* **61** (2000), 054015.
[8] P. Niezurawski, A. F. Zarnecki and M. Krawczyk, *Study of the Higgs boson decays into W+ W- and ZZ at the photon collider*, *JHEP* **11** (2002), 034.
[9] R. M. Godbole, S. D. Rindani and R. K. Singh, *Study of CP property of the Higgs at a photon collider using $\gamma\vec{\gamma}t\bar{t} \to lX$*, *Phys. Rev. D* **67** (2003), 095009.
[10] T. G. Rizzo, *New physics beyond the standard model at gamma gamma colliders*, *Nucl. Instrum. Meth. A* **472** (2001) 37.
[11] L. Resnick, M. K. Sundaresan and P. J. S. Watson, *Is there a light scalar Boson? Phys. Rev. D* **8** (1973) 172.
[12] M. A. Shifman, A. I. Vainshtein, M. B. Voloshin and V. I. Zakharov, *1465 low-energy theorems for Higgs Boson couplings to photons Sov. J. Nucl. Phys.* **30** (1979) 711 [*Yad. Fiz.* **30** (1979) 1368].
[13] R. Gastmans, S. L. Wu and T. T. Wu, *Higgs decay $H \to \gamma\gamma$ through a W loop: difficulty with dimensional regularization* arXiv:1108.5322 [hep-ph].
[14] R. Gastmans, S. L. Wu and T. T. Wu, *Higgs decay into two photons, revisited*, arXiv:1108.5872 [hep-ph]
[15] T. T. Wu and S. L. Wu, *Failure of the Feynman R_1 gauge for the standard model: an explicit example Int. J. Mod. Phys. A* **31** (2016) no.04n05, 1650028.
[16] M. Shifman, A. Vainshtein, M. B. Voloshin and V. Zakharov, *Higgs boson decay into two photons through the W-boson loop: No decoupling in the mW $\to 0$ limit*, *Phys. Rev. D* **85** (2012) 013015.
[17] D. Huang, Y. Tang and Y. L. Wu, *Note on Higgs Decay into two photons $H \to \gamma\gamma$*, *Commun. Theor. Phys.* **57** (2012) 427.
[18] W. J. Marciano, C. Zhang and S. Willenbrock, *Higgs decay to two photons*, *Phys. Rev. D* **85** (2012) 013002.
[19] F. Jegerlehner, *Comment on $H --> \gamma\gamma$ and the role of the decoupling theorem and the equivalence theorem*, arXiv:1110.0869 [hep-ph].
[20] H. S. Shao, Y. J. Zhang and K. T. Chao, *Reduction schemes in cutoff regularization and Higgs decay into two photons*, *JHEP* **1201** (2012) 053.
[21] A. M. Donati and R. Pittau, *Gauge invariance at work in FDR: $H \to \gamma\gamma$ JHEP* **1304** (2013) 167.
[22] E. Christova and I. Todorov, *Once more on the W-Loop contribution to the Higgs decay into two photons Bulg. J. Phys.* **42** (2015) 296.
[23] J. Kile, *$H \to \gamma\gamma$, gauge invariance, and the hierarchy problem*, *Int. J. Mod. Phys. A* **31** (2016) 1630046.
[24] S. Y. Li, Z. G. Si and X. F. Zhang, *Cancellation of divergences in unitary gauge calculation of $H \to \gamma\gamma$ process via one W loop, and application*, arXiv:1705.04941 [hep-ph].
[25] K. Melnikov and A. Vainshtein, *Higgs boson decay to two photons and dispersion relations*, *Phys. Rev. D* **93** (2016) no.5, 053015.
[26] T. T. Wu and S. L. Wu, *Comparing the R_ξ gauge and the unitary gauge for the standard model: an example*, *Nucl. Phys. B* **914** (2017) 421.
[27] J. Gegelia and U. G. Meißner, *Once more on the Higgs decay into two photons*, *Nucl. Phys. B* **934** (2018) 1.
[28] T. Hahn and M. Perez-Victoria, *Automatized one loop calculations in four-dimensions and D-dimensions*, *Comput. Phys. Commun.* **118** (1999) 153.
[29] A. Denner and S. Dittmaier, *Reduction schemes for one-loop tensor integrals*, *Nucl. Phys. B* **734** (2006) 62.
[30] H. H. Patel, *Package-X: A Mathematica package for the analytic calculation of one-loop integrals*, *Comput. Phys. Commun.* **197** (2015) 276.

Appendix A: One-loop form factors for $H \to \gamma\gamma^*$

Analytical results for one off-shell photon in the decay of $H \to \gamma\gamma^*$ are reported in this subsection. Due to the fermion loop contributions, the form factors are shown

$$\begin{aligned}\mathscr{A}_{00}^{(f)} &= -4m_f^2 N_C Q_f^2 \Big\{ \mathbf{B}_0\left(M_H^2; m_f^2, m_f^2\right) - 4\mathbf{C}_{00}\left(M_H^2, 0, p_2^2; m_f^2, m_f^2, m_f^2\right) \\ &\quad + \frac{M_H^2 - p_2^2}{2} \mathbf{C}_0\left(M_H^2, 0, p_2^2; m_f^2, m_f^2, m_f^2\right) \Big\}, \end{aligned} \tag{34}$$

$$\begin{aligned}\mathscr{A}_{21}^{(f)} &= 4m_f^2 N_C Q_f^2 \Big\{ 4\Big[\mathbf{C}_{12}\left(M_H^2, 0, p_2^2; m_f^2, m_f^2, m_f^2\right) + \mathbf{C}_{11}\left(M_H^2, 0, p_2^2; m_f^2, m_f^2, m_f^2\right) \\ &\quad + \mathbf{C}_1\left(M_H^2, 0, p_2^2; m_f^2, m_f^2, m_f^2\right) \Big] + \mathbf{C}_0\left(M_H^2, 0, p_2^2; m_f^2, m_f^2, m_f^2\right) \Big\}. \end{aligned} \tag{35}$$

Applying the same procedure, the form factors calculating from W boson loop diagrams are expressed as follows

$$\begin{aligned}\mathscr{A}_{00}^{(W)} &= M_W^2 \Big\{ \mathbf{B}_0\left(p_2^2; M_W^2, M_W^2\right) + 8\left[p_2^2 - M_H^2\right] \mathbf{C}_0\left(0, p_2^2, M_H^2; M_W^2, M_W^2, M_W^2\right) \Big\} \\ &\quad - \left[M_H^2 + 2(d-1)M_W^2\right] \Big[\mathbf{B}_0\left(M_H^2; M_W^2, M_W^2\right) - 4\mathbf{C}_{00}\left(0, p_2^2, M_H^2; M_W^2, M_W^2, M_W^2\right) \Big] \\ &\quad - M_W^2 \mathbf{B}_0(0; M_W^2, M_W^2) \end{aligned} \tag{36}$$

$$\begin{aligned}\mathscr{A}_{21}^{(W)} &= 2M_W^2 \Big\{ 4(d-1)\Big[\mathbf{C}_{22}\left(0, p_2^2, M_H^2; M_W^2, M_W^2, M_W^2\right) + \mathbf{C}_{12}\left(0, p_2^2, M_H^2; M_W^2, M_W^2, M_W^2\right) \Big] \\ &\quad + 2(2d+1)\mathbf{C}_2\left(0, p_2^2, M_H^2; M_W^2, M_W^2, M_W^2\right) + 11\mathbf{C}_0\left(0, p_2^2, M_H^2; M_W^2, M_W^2, M_W^2\right) \\ &\quad + 3\mathbf{C}_1\left(0, p_2^2, M_H^2; M_W^2, M_W^2, M_W^2\right) \Big\} + 4M_H^2 \Big\{ \mathbf{C}_{22}\left(0, p_2^2, M_H^2; M_W^2, M_W^2, M_W^2\right) \\ &\quad + \mathbf{C}_{12}\left(0, p_2^2, M_H^2; M_W^2, M_W^2, M_W^2\right) + \mathbf{C}_2\left(0, p_2^2, M_H^2; M_W^2, M_W^2, M_W^2\right) \Big\}. \end{aligned} \tag{37}$$

Further, one-loop form factors for this channel with contributing of charged scalars in the loop diagrams are obtained

$$\mathscr{A}_{00}^{(S_i)} = -2\Big\{ \mathbf{B}_0\left(M_H^2; M_{S_i}^2, M_{S_i}^2\right) - 4\mathbf{C}_{00}\left(M_H^2, 0, p_2^2; M_{S_i}^2, M_{S_i}^2, M_{S_i}^2\right) \Big\}, \tag{38}$$

$$\begin{aligned}\mathscr{A}_{21}^{(S_i)} &= 8\Big\{ \mathbf{C}_{12}\left(M_H^2, 0, p_2^2; M_{S_i}^2, M_{S_i}^2, M_{S_i}^2\right) + \mathbf{C}_{11}\left(M_H^2, 0, p_2^2; M_{S_i}^2, M_{S_i}^2, M_{S_i}^2\right) \\ &\quad + \mathbf{C}_1\left(M_H^2, 0, p_2^2; M_{S_i}^2, M_{S_i}^2, M_{S_i}^2\right) \Big\}. \end{aligned} \tag{39}$$

We find that all form factors in this subsection can be obtained by taking $p_1^2 \to 0$ from the results in two off-shell photons.

Appendix B: Feynman rules for $H \to \gamma\gamma$ in R_ξ gauge

Feynman rules for $H \to \gamma\gamma$ in R_ξ gauge devoted in this appendix.

Table 2. Feynman rules involving the decay $H \to \gamma\gamma$ through fermion and W boson, charged scalar loop diagrams in the R_ξ gauge.

Particle types	Propagators
Fermions	$\frac{i(\not{p}+m_f)}{p^2-m_f^2}$
W boson	$\frac{-i}{p^2-M_W^2}\left[g^{\mu\nu}-(1-\xi)\frac{p^\mu p^\nu}{p^2-M_\xi^2}\right]$
Goldstone boson	$\frac{i}{p^2-M_\xi^2}$
Ghost	$\frac{i}{p^2-M_\xi^2}$
Charged scalar	$\frac{i}{p^2-M_{S_i}^2}$

Table 3. Couplings involving the decay $H \to \gamma\gamma$ through fermion and W boson, charged scalar loops in the R_ξ gauge with the short notation for the standard Lorentz tensors of the gauge boson self couplings $\Gamma_{\mu\nu\lambda}(p_1,p_2,p_3) = g_{\mu\nu}(p_1-p_2)_\lambda + g_{\lambda\nu}(p_2-p_3)_\mu + g_{\mu\lambda}(p_3-p_1)_\nu$ and $S_{\mu\nu,\alpha\beta} = 2g_{\mu\nu}g_{\alpha\beta} - g_{\mu\alpha}g_{\nu\beta} - g_{\mu\beta}g_{\nu\alpha}$.

Vertices	Couplings
$A_\mu f\bar{f}$	$ieQ_f\gamma_\mu$
$Hf\bar{f}$	$-igm_f/(2M_W)$
$H\cdot W_\mu\cdot W_\nu$	$igM_W g_{\mu\nu}$
$A_\mu(p_1)\cdot W_\nu^+(p_2)\cdot W_\lambda^-(p_3)$	$-ie\Gamma_{\mu\nu\lambda}(p_1,p_2,p_3)$
$A_\mu\cdot A_\nu\cdot W_\alpha^+\cdot W_\beta^-$	$-ie^2S_{\mu\nu,\alpha\beta}$
$H(p_1)\cdot W_\mu\cdot\chi(p_2)$	$-i\frac{g}{2}(p_2-p_1)_\mu$
$A_\mu\cdot W_\nu\cdot\chi$	$-ieM_W g_{\mu\nu}$
$H\cdot\chi\cdot\chi$	$-igM_H^2/(2M_W)$
$A_\mu\cdot\chi(p_1)\cdot\chi(p_2)$	$-ie(p_2-p_1)_\mu$
$A_\mu\cdot A_\nu\cdot\chi\cdot\chi$	$i2e^2g_{\mu\nu}$
$H\cdot A_\mu\cdot W_\nu\cdot\chi$	$-ie\frac{g}{2}g_{\mu\nu}$
$H\cdot c\cdot c$	$-i\xi\frac{g}{2}M_W$
$A_\mu\cdot c\cdot c$	$-iep_\mu$
$HS_i\bar{S}_i$	$i\lambda_{HS_i\bar{S}_i}$
$A_\mu S_i(q_1)\bar{S}_i(q_2)$	$ieQ_{S_i}(q_2-q_1)_\mu$
$A_\mu A_\nu S_i\bar{S}_i$	$2ie^2Q_{S_i}^2g_{\mu\nu}$

Appendix C: Amplitude $H \to \gamma\gamma$ in R_ξ gauge

One-loop Feynman amplitudes for the process $H \to \gamma\gamma$ in R_ξ gauge are shown in this appendix. For fermion loop diagrams, one has

$$\mathscr{A}_{(1+2)}^{(\text{fermion})} = \frac{gm_fQ_f^2e^2}{M_W}\int\frac{\mathrm{d}^dk}{(2\pi)^d}\,\frac{\mathrm{Tr}\{(\not{k}+m_f)\gamma^\mu(\not{k}-\not{p}_1+m_f)\gamma^\nu(\not{k}-\not{p}+m_f)\}}{(k^2-m_f^2)[(k-p_1)^2-m_f^2][(k-p)^2-m_f^2]}\varepsilon_\mu^*(p_1)\varepsilon_\nu^*(p_2). \tag{40}$$

We next show Feynman amplitude for W boson loop diagrams

Diagram *a*

The Feynman amplitude for W boson loop diagrams are decomposed into 8 terms as follows:

$$\begin{aligned}\mathscr{A}^{(a)}(\xi) &= \mathscr{A}_{111}(\xi)+\mathscr{A}_{112}(\xi)+\mathscr{A}_{121}(\xi)+\mathscr{A}_{211}(\xi)\\ &\quad +\mathscr{A}_{122}(\xi)+\mathscr{A}_{212}(\xi)+\mathscr{A}_{221}(\xi)+\mathscr{A}_{222}(\xi).\end{aligned} \tag{41}$$

Where $\mathscr{A}_{111}(\xi),\cdots,\mathscr{A}_{222}(\xi)$ are corresponding to which term in the right hand side of Eq. (14) is taken. These terms are written

$$\begin{aligned}\mathscr{A}_{111}(\xi) &= 2e^2gM_W\int\frac{\mathrm{d}^dk}{(2\pi)^d}\,g_{\alpha\beta}\Gamma_{\mu\tau\lambda}(-p_1,k,-k+p_1)\Gamma_{\nu\rho\delta}(-p_2,k-p_1,-k+p)\,\epsilon^*_\mu(p_1)\epsilon^*_\nu(p_2)\\ &\quad\times\frac{g^{\alpha\tau}-k^\alpha k^\tau/M_W^2}{k^2-M_W^2}\,\frac{g^{\lambda\rho}-(k-p_1)^\lambda(k-p_1)^\rho/M_W^2}{(k-p_1)^2-M_W^2}\,\frac{g^{\beta\delta}-(k-p)^\beta(k-p)^\delta/M_W^2}{(k-p)^2-M_W^2},\end{aligned} \tag{42}$$

$$\begin{aligned}\mathscr{A}_{112}(\xi) &= 2e^2gM_W\int\frac{\mathrm{d}^dk}{(2\pi)^d}\,g_{\alpha\beta}\Gamma_{\mu\tau\lambda}(-p_1,k,-k+p_1)\Gamma_{\nu\rho\delta}(-p_2,k-p_1,-k+p)\,\epsilon^*_\mu(p_1)\epsilon^*_\nu(p_2)\\ &\quad\times\frac{g^{\alpha\tau}-k^\alpha k^\tau/M_W^2}{k^2-M_W^2}\,\frac{g^{\lambda\rho}-(k-p_1)^\lambda(k-p_1)^\rho/M_W^2}{(k-p_1)^2-M_W^2}\,\frac{(k-p)^\beta(k-p)^\delta/M_W^2}{(k-p)^2-M_\xi^2},\end{aligned} \tag{43}$$

$$\begin{aligned}\mathscr{A}_{121}(\xi) &= 2e^2gM_W\int\frac{\mathrm{d}^dk}{(2\pi)^d}\,g_{\alpha\beta}\Gamma_{\mu\tau\lambda}(-p_1,k,-k+p_1)\Gamma_{\nu\rho\delta}(-p_2,k-p_1,-k+p)\,\epsilon^*_\mu(p_1)\epsilon^*_\nu(p_2)\\ &\quad\times\frac{g^{\alpha\tau}-k^\alpha k^\tau/M_W^2}{k^2-M_W^2}\,\frac{(k-p_1)^\lambda(k-p_1)^\rho/M_W^2}{(k-p_1)^2-M_\xi^2}\,\frac{g^{\beta\delta}-(k-p)^\beta(k-p)^\delta/M_W^2}{(k-p)^2-M_W^2},\end{aligned} \tag{44}$$

$$\begin{aligned}\mathscr{A}_{211}(\xi) &= 2e^2gM_W\int\frac{\mathrm{d}^dk}{(2\pi)^d}\,g_{\alpha\beta}\Gamma_{\mu\tau\lambda}(-p_1,k,-k+p_1)\Gamma_{\nu\rho\delta}(-p_2,k-p_1,-k+p)\,\epsilon^*_\mu(p_1)\epsilon^*_\nu(p_2)\\ &\quad\times\frac{k^\alpha k^\tau/M_W^2}{k^2-M_\xi^2}\,\frac{g^{\lambda\rho}-(k-p_1)^\lambda(k-p_1)^\rho/M_W^2}{(k-p_1)^2-M_W^2}\,\frac{g^{\beta\delta}-(k-p)^\beta(k-p)^\delta/M_W^2}{(k-p)^2-M_W^2}\end{aligned} \tag{45}$$

$$\begin{aligned}\mathscr{A}_{122}(\xi) &= 2e^2gM_W\int\frac{\mathrm{d}^dk}{(2\pi)^d}\,g_{\alpha\beta}\Gamma_{\mu\tau\lambda}(-p_1,k,-k+p_1)\Gamma_{\nu\rho\delta}(-p_2,k-p_1,-k+p)\,\epsilon^*_\mu(p_1)\epsilon^*_\nu(p_2)\\ &\quad\times\frac{g^{\alpha\tau}-k^\alpha k^\tau/M_W^2}{k^2-M_W^2}\,\frac{(k-p_1)^\lambda(k-p_1)^\rho/M_W^2}{(k-p_1)^2-M_\xi^2}\,\frac{(k-p)^\beta(k-p)^\delta/M_W^2}{(k-p)^2-M_\xi^2},\end{aligned} \tag{46}$$

$$\begin{aligned}\mathscr{A}_{212}(\xi) &= 2e^2 g M_W \int \frac{\mathrm{d}^d k}{(2\pi)^d}\, g_{\alpha\beta}\Gamma_{\mu\tau\lambda}(-p_1,k,-k+p_1)\Gamma_{\nu\rho\delta}(-p_2,k-p_1,-k+p)\,\epsilon^*_\mu(p_1)\epsilon^*_\nu(p_2)\\ &\quad\times \frac{k^\alpha k^\tau/M_W^2}{k^2-M_\xi^2}\,\frac{g^{\lambda\rho}-(k-p_1)^\lambda(k-p_1)^\rho/M_W^2}{(k-p_1)^2-M_W^2}\,\frac{(k-p)^\beta(k-p)^\delta/M_W^2}{(k-p)^2-M_\xi^2}, \end{aligned} \tag{47}$$

$$\begin{aligned}\mathscr{A}_{221}(\xi) &= 2e^2 g M_W \int \frac{\mathrm{d}^d k}{(2\pi)^d}\, g_{\alpha\beta}\Gamma_{\mu\tau\lambda}(-p_1,k,-k+p_1)\Gamma_{\nu\rho\delta}(-p_2,k-p_1,-k+p)\,\epsilon^*_\mu(p_1)\epsilon^*_\nu(p_2)\\ &\quad\times \frac{k^\alpha k^\tau/M_W^2}{k^2-M_\xi^2}\,\frac{(k-p_1)^\lambda(k-p_1)^\rho/M_W^2}{(k-p_1)^2-M_\xi^2}\,\frac{g^{\beta\delta}-(k-p)^\beta(k-p)^\delta/M_W^2}{(k-p)^2-M_W^2}, \end{aligned} \tag{48}$$

$$\begin{aligned}\mathscr{A}_{222}(\xi) &= 2e^2 g M_W \int \frac{\mathrm{d}^d k}{(2\pi)^d}\, g_{\alpha\beta}\Gamma_{\mu\tau\lambda}(-p_1,k,-k+p_1)\Gamma_{\nu\rho\delta}(-p_2,k-p_1,-k+p)\,\epsilon^*_\mu(p_1)\epsilon^*_\nu(p_2)\\ &\quad\times \frac{k^\alpha k^\tau/M_W^2}{k^2-M_\xi^2}\,\frac{(k-p_1)^\lambda(k-p_1)^\rho/M_W^2}{(k-p_1)^2-M_\xi^2}\,\frac{(k-p)^\beta(k-p)^\delta/M_W^2}{(k-p)^2-M_\xi^2}. \end{aligned} \tag{49}$$

Diagram *b*

$$\mathscr{A}^{(b)}(\xi) = \mathscr{A}_{11}(\xi)+\mathscr{A}_{12}(\xi)+\mathscr{A}_{21}(\xi)+\mathscr{A}_{22}(\xi) \tag{50}$$

where

$$\begin{aligned}\mathscr{A}_{11}(\xi) &= -e^2 g M_W \int \frac{\mathrm{d}^d k}{(2\pi)^d}\, g_{\alpha\beta} S_{\mu\nu,\lambda\rho}\,\epsilon^*_\mu(p_1)\epsilon^*_\nu(p_2)\\ &\quad\times \frac{g^{\alpha\lambda}-k^\alpha k^\lambda/M_W^2}{k^2-M_W^2}\,\frac{g^{\beta\rho}-(k-p)^\beta(k-p)^\rho/M_W^2}{(k-p)^2-M_W^2}, \end{aligned} \tag{51}$$

$$\begin{aligned}\mathscr{A}_{12}(\xi) &= -e^2 g M_W \int \frac{\mathrm{d}^d k}{(2\pi)^d}\, g_{\alpha\beta} S_{\mu\nu,\lambda\rho}\,\epsilon^*_\mu(p_1)\epsilon^*_\nu(p_2)\\ &\quad\times \frac{g^{\alpha\lambda}-k^\alpha k^\lambda/M_W^2}{k^2-M_W^2}\,\frac{(k-p)^\beta(k-p)^\rho/M_W^2}{(k-p)^2-M_\xi^2}, \end{aligned} \tag{52}$$

$$\begin{aligned}\mathscr{A}_{21}(\xi) &= -e^2 g M_W \int \frac{\mathrm{d}^d k}{(2\pi)^d}\, g_{\alpha\beta} S_{\mu\nu,\lambda\rho}\,\epsilon^*_\mu(p_1)\epsilon^*_\nu(p_2)\\ &\quad\times \frac{k^\alpha k^\lambda/M_W^2}{k^2-M_\xi^2}\,\frac{g^{\beta\rho}-(k-p)^\beta(k-p)^\rho/M_W^2}{(k-p)^2-M_W^2}, \end{aligned} \tag{53}$$

$$\begin{aligned}\mathscr{A}_{22}(\xi) &= -e^2 g M_W \int \frac{\mathrm{d}^d k}{(2\pi)^d}\, g_{\alpha\beta} S_{\mu\nu,\lambda\rho}\,\epsilon^*_\mu(p_1)\epsilon^*_\nu(p_2)\\ &\quad\times \frac{k^\alpha k^\lambda/M_W^2}{k^2-M_\xi^2}\,\frac{(k-p)^\beta(k-p)^\rho/M_W^2}{(k-p)^2-M_\xi^2}. \end{aligned} \tag{54}$$

Diagram *c*

$$\mathscr{A}^{(c)}(\xi) = \mathscr{A}_{110}(\xi)+\mathscr{A}_{120}(\xi)+\mathscr{A}_{210}(\xi)+\mathscr{A}_{220}(\xi) \tag{55}$$

where

$$\begin{aligned}\mathscr{A}_{110}(\xi) &= 2e^2 gM_W \int \frac{\mathrm{d}^d k}{(2\pi)^d}(k-2p)_\alpha g_{\nu\rho}\Gamma_{\mu\tau\lambda}(-p_1,k,-k+p_1)\,\epsilon^*_\mu(p_1)\epsilon^*_\nu(p_2)\\ &\times\frac{g^{\alpha\tau}-k^\alpha k^\tau/M_W^2}{k^2-M_W^2}\,\frac{g^{\lambda\rho}-(k-p_1)^\lambda(k-p_1)^\rho/M_W^2}{(k-p_1)^2-M_W^2}\,\frac{1}{(k-p)^2-M_\xi^2},\end{aligned} \tag{56}$$

$$\begin{aligned}\mathscr{A}_{120}(\xi) &= 2e^2 gM_W \int \frac{\mathrm{d}^d k}{(2\pi)^d}(k-2p)_\alpha g_{\nu\rho}\Gamma_{\mu\tau\lambda}(-p_1,k,-k+p_1)\,\epsilon^*_\mu(p_1)\epsilon^*_\nu(p_2)\\ &\times\frac{g^{\alpha\tau}-k^\alpha k^\tau/M_W^2}{k^2-M_W^2}\,\frac{(k-p_1)^\lambda(k-p_1)^\rho/M_W^2}{(k-p_1)^2-M_\xi^2}\,\frac{1}{(k-p)^2-M_\xi^2},\end{aligned} \tag{57}$$

$$\begin{aligned}\mathscr{A}_{210}(\xi) &= 2e^2 gM_W \int \frac{\mathrm{d}^d k}{(2\pi)^d}(k-2p)_\alpha g_{\nu\rho}\Gamma_{\mu\tau\lambda}(-p_1,k,-k+p_1)\,\epsilon^*_\mu(p_1)\epsilon^*_\nu(p_2)\\ &\times\frac{k^\alpha k^\tau/M_W^2}{k^2-M_\xi^2}\,\frac{g^{\lambda\rho}-(k-p_1)^\lambda(k-p_1)^\rho/M_W^2}{(k-p_1)^2-M_W^2}\,\frac{1}{(k-p)^2-M_\xi^2},\end{aligned} \tag{58}$$

$$\begin{aligned}\mathscr{A}_{220}(\xi) &= 2e^2 gM_W \int \frac{\mathrm{d}^d k}{(2\pi)^d}(k-2p)_\alpha g_{\nu\rho}\Gamma_{\mu\tau\lambda}(-p_1,k,-k+p_1)\,\epsilon^*_\mu(p_1)\epsilon^*_\nu(p_2)\\ &\times\frac{k^\alpha k^\tau/M_W^2}{k^2-M_\xi^2}\,\frac{(k-p_1)^\lambda(k-p_1)^\rho/M_W^2}{(k-p_1)^2-M_\xi^2}\,\frac{1}{(k-p)^2-M_\xi^2}.\end{aligned} \tag{59}$$

Diagram *d*

$$\mathscr{A}^{(d)}(\xi) = \mathscr{A}_{10}(\xi)+\mathscr{A}_{20}(\xi) \tag{60}$$

where

$$\mathscr{A}_{10}(\xi) = -2e^2 gM_W \int \frac{\mathrm{d}^d k}{(2\pi)^d} g_{\mu\lambda}g_{\nu\rho}\frac{g^{\lambda\rho}-(k-p_1)^\lambda(k-p_1)^\rho/M_W^2}{(k-p_1)^2-M_W^2}\,\frac{\epsilon^*_\mu(p_1)\epsilon^*_\nu(p_2)}{(k-p)^2-M_\xi^2}, \tag{61}$$

$$\mathscr{A}_{20}(\xi) = -2e^2 gM_W \int \frac{\mathrm{d}^d k}{(2\pi)^d} g_{\mu\lambda}g_{\nu\rho}\frac{(k-p_1)^\lambda(k-p_1)^\rho/M_W^2}{(k-p_1)^2-M_\xi^2}\,\frac{\epsilon^*_\mu(p_1)\epsilon^*_\nu(p_2)}{(k-p)^2-M_\xi^2}. \tag{62}$$

Diagram *e*

$$\mathscr{A}^{(e)}(\xi) = \mathscr{A}_{100}(\xi)+\mathscr{A}_{200}(\xi) \tag{63}$$

where

$$\mathscr{A}_{100}(\xi) = -2e^2 g M_W \int \frac{d^d k}{(2\pi)^d} g_{\mu\tau}(k-2p)_\alpha(-2k+2p_1+p_2)_\nu \times \frac{g^{\alpha\tau}-k^\alpha k^\tau/M_W^2}{k^2-M_W^2}\frac{1}{(k-p_1)^2-M_\xi^2}\frac{1}{(k-p)^2-M_\xi^2}\epsilon^*_\mu(p_1)\epsilon^*_\nu(p_2), \quad (64)$$

$$\mathscr{A}_{200}(\xi) = -2e^2 g M_W \int \frac{d^d k}{(2\pi)^d} g_{\mu\tau}(k-2p)_\alpha(-2k+2p_1+p_2)_\nu \times \frac{k^\alpha k^\tau/M_W^2}{k^2-M_\xi^2}\frac{1}{(k-p_1)^2-M_\xi^2}\frac{1}{(k-p)^2-M_\xi^2}\epsilon^*_\mu(p_1)\epsilon^*_\nu(p_2). \quad (65)$$

Diagram f

$$\mathscr{A}^{(f)}(\xi) = \mathscr{A}_{101}(\xi)+\mathscr{A}_{102}(\xi)+\mathscr{A}_{201}(\xi)+\mathscr{A}_{202}(\xi) \quad (66)$$

where

$$\mathscr{A}_{101}(\xi) = -2e^2 g M_W^3 \int \frac{d^d k}{(2\pi)^d} g_{\alpha\beta}g_{\mu\tau}g_{\nu\delta}\,\epsilon^*_\mu(p_1)\epsilon^*_\nu(p_2) \times \frac{g^{\alpha\tau}-k^\alpha k^\tau/M_W^2}{k^2-M_W^2}\frac{1}{(k-p_1)^2-M_\xi^2}\frac{g^{\beta\delta}-(k-p)^\beta(k-p)^\delta/M_W^2}{(k-p)^2-M_W^2}, \quad (67)$$

$$\mathscr{A}_{102}(\xi) = -2e^2 g M_W^3 \int \frac{d^d k}{(2\pi)^d} g_{\alpha\beta}g_{\mu\tau}g_{\nu\delta}\,\epsilon^*_\mu(p_1)\epsilon^*_\nu(p_2) \times \frac{g^{\alpha\tau}-k^\alpha k^\tau/M_W^2}{k^2-M_W^2}\frac{1}{(k-p_1)^2-M_\xi^2}\frac{(k-p)^\beta(k-p)^\delta/M_W^2}{(k-p)^2-M_\xi^2}, \quad (68)$$

$$\mathscr{A}_{201}(\xi) = -2e^2 g M_W^3 \int \frac{d^d k}{(2\pi)^d} g_{\alpha\beta}g_{\mu\tau}g_{\nu\delta}\,\epsilon^*_\mu(p_1)\epsilon^*_\nu(p_2) \times \frac{k^\alpha k^\tau/M_W^2}{k^2-M_\xi^2}\frac{1}{(k-p_1)^2-M_\xi^2}\frac{g^{\beta\delta}-(k-p)^\beta(k-p)^\delta/M_W^2}{(k-p)^2-M_W^2}, \quad (69)$$

$$\mathscr{A}_{202}(\xi) = -2e^2 g M_W^3 \int \frac{d^d k}{(2\pi)^d} g_{\alpha\beta}g_{\mu\tau}g_{\nu\delta}\,\epsilon^*_\mu(p_1)\epsilon^*_\nu(p_2) \times \frac{k^\alpha k^\tau/M_W^2}{k^2-M_\xi^2}\frac{1}{(k-p_1)^2-M_\xi^2}\frac{(k-p)^\beta(k-p)^\delta/M_W^2}{(k-p)^2-M_\xi^2}. \quad (70)$$

Diagram g

$$\mathscr{A}^{(g)}(\xi) = \mathscr{A}_{010}(\xi)+\mathscr{A}_{020}(\xi) \quad (71)$$

where

$$\mathscr{A}_{010}(\xi) = -e^2 g M_H^2 M_W \int \frac{\mathrm{d}^d k}{(2\pi)^d} g_{\mu\lambda} g_{\nu\rho} \epsilon_\mu^*(p_1)\epsilon_\nu^*(p_2) \times \frac{1}{k^2 - M_\xi^2} \frac{g^{\lambda\rho} - (k-p_1)^\lambda (k-p_1)^\rho / M_W^2}{(k-p_1)^2 - M_W^2} \frac{1}{(k-p)^2 - M_\xi^2}, \quad (72)$$

$$\mathscr{A}_{020}(\xi) = -e^2 g M_H^2 M_W \int \frac{\mathrm{d}^d k}{(2\pi)^d} g_{\mu\lambda} g_{\nu\rho} \epsilon_\mu^*(p_1)\epsilon_\nu^*(p_2) \times \frac{1}{k^2 - M_\xi^2} \frac{(k-p_1)^\lambda (k-p_1)^\rho / M_W^2}{(k-p_1)^2 - M_\xi^2} \frac{1}{(k-p)^2 - M_\xi^2}. \quad (73)$$

Diagram *h*

$$\mathscr{A}^{(h)}(\xi) = e^2 g \frac{M_H^2}{M_W} \int \frac{\mathrm{d}^d k}{(2\pi)^d} (-2k+p_1)_\mu (-2k+2p_1+p_2)_\nu \times \frac{1}{k^2 - M_\xi^2} \frac{1}{(k-p_1)^2 - M_\xi^2} \frac{1}{(k-p)^2 - M_\xi^2} \epsilon_\mu^*(p_1)\epsilon_\nu^*(p_2). \quad (74)$$

Diagram *i*

$$\mathscr{A}^{(i)}(\xi) = -e^2 g \frac{M_H^2}{M_W} \int \frac{\mathrm{d}^d k}{(2\pi)^d} g_{\mu\nu} \frac{1}{k^2 - M_\xi^2} \frac{1}{(k-p)^2 - M_\xi^2} \epsilon_\mu^*(p_1)\epsilon_\nu^*(p_2). \quad (75)$$

Diagram *j*

$$\mathscr{A}^{(j)}(\xi) = -2e^2 g M_W \xi \int \frac{\mathrm{d}^d k}{(2\pi)^d} (k-p_1)_\mu (k-p)_\nu \times \frac{1}{k^2 - M_\xi^2} \frac{1}{(k-p_1)^2 - M_\xi^2} \frac{1}{(k-p)^2 - M_\xi^2} \epsilon_\mu^*(p_1)\epsilon_\nu^*(p_2). \quad (76)$$

Feynman amplitude due to the charged scalar particles exchanging in the loop diagrams reads

$$\mathscr{A}_{(1)}^{(S_i)} = -2e^2 Q_{S_i}^2 \lambda_{HS_i\bar{S}_i} \int \frac{\mathrm{d}^d k}{(2\pi)^d} (-2k+p_1)_\mu (-2k+2p_1+p_2)_\nu \times \frac{1}{k^2 - M_{S_i}^2} \frac{1}{(k-p_1)^2 - M_{S_i}^2} \frac{1}{(k-p)^2 - M_{S_i}^2} \epsilon_\mu^*(p_1)\epsilon_\nu^*(p_2), \quad (77)$$

$$\mathscr{A}_{(2)}^{(S_i)} = 2e^2 Q_{S_i}^2 \lambda_{HS_i\bar{S}_i} \int \frac{\mathrm{d}^d k}{(2\pi)^d} g_{\mu\nu} \frac{1}{k^2 - M_{S_i}^2} \frac{1}{(k-p)^2 - M_{S_i}^2} \epsilon_\mu^*(p_1)\epsilon_\nu^*(p_2). \quad (78)$$